Subtractive modelling using the reverse Condensed Transfer Function method: influence of the numerical errors

Florent Dumortier, Laurent Maxit, Valentin Meyer

inter·noise 2021
1–5 August | Washington, DC

Subtractive modelling using the reverse Condensed Transfer Function method: influence of the numerical errors

Florent Dumortier[1]
Univ Lyon, INSA Lyon, LVA, EA677
25bis av. Jean Capelle, 69621 Villeurbanne, France

Laurent Maxit[2]
Univ Lyon, INSA Lyon, LVA, EA677
25bis av. Jean Capelle, 69621 Villeurbanne, France

Valentin Meyer[3]
Naval Group Research
199 av. Pierre-Gilles de Gennes, 83190 Ollioules, France

ABSTRACT

Decoupling procedures based on substructuring methods allow to predict the vibroacoustic behaviour of a given system by removing a part of an original system that can be easily modelled. The reverse Condensed Transfer Function (rCTF) method has been developed to decouple acoustical or mechanical subsystems that are coupled along lines or surfaces. From the so-called condensed transfer functions (CTFs) of the original system and of the removed part, the behaviour of the system of interest can be predicted. The theoretical framework as well as a numerical validation have been recently published. In the present paper, we focus on the influence of numerical errors on the results of the rCTF method, when the CTFs are calculated using numerical models for the original system and the removed part. The rCTF method is applied to a test case consisting in the scattering problem of a rigid sphere in an infinite water domain and impacted by an acoustic plane wave. Discrete green formulation and finite element method are used to estimate the CTFs. Numerical results will be presented in order to evaluate the sensitivity of the method to model errors and the potential promises and limitations of the method will be highlighted.

1. INTRODUCTION

Today, numerical methods in vibrations, acoustics and vibroacoustics are widely used in the industry to design products meeting strong noise and vibration requirements. In these domains, substructuring methods have emerged to circumvent prohibitive calculation costs that can be met at mid and high

[1]florent.dumortier@insa-lyon.fr

[2]laurent.maxit@insa-lyon.fr

[3]valentin.meyer@naval-group.com

frequencies. Among these methods, admittance and impedance concepts have been derived as an analogy between electrical and mechanical systems [1]. These methods, based on frequency transfer functions, allow one to study complex systems by dividing them into subsystems for which the transfer functions are evaluated by different means (analytical, numerical or experimental). A first formulation, based on point-coupled mechanical subsystems, has been derived by Rubin [2] and O'Hara [3]. The approach was extended to multi-point coupled structures by Petersson and Plunt [4] and to weakly coupled structural-acoustic systems by Kim and Brennan [5].

The approach was then extended to surface-coupled subsystems via the Patch Transfer Function (PTF) method, initially developped to couple two acoustic domains [6]. The interface between the two domains is decomposed into patches that are defined using a wavelength-based criterion. This method was highly studied over the past years for industrial applications such as automotive [7] and naval [8] domains, and the convergence of the method was improved by partitioning the subsystems outside the acoustic near field of the structures [8] and by introducing residual mode shapes in the modal expansion of the Patch Transfer Functions [9]. As a generalization of the PTF method, the Condensed Transfer Function (CTF) method was introduced to study linear vibro-acoustic problems coupled along lines or surfaces [10]. Condensation functions, that can take numerous forms (patches, but also complex exponentials or Chebyshev polynomials) are used as a basis for evaluating the forces and displacements at the junctions. This method can find industrial applications, for example in the naval domain, where it has been used to predict the vibroacoustic behaviour of stiffened cylindrical shells coupled to non-axisymmetric internal structures [11].

More recently, a reverse formulation of the CTF (rCTF) method has been developped by the authors in order to remove a subsystem from a global system [12]. Such an approach can be interesting to model the effect of a default or a void in a complex structure. Similar decoupling techniques have already been studied in the past, in experimental studies to estimate the impedances of a part of a system [13, 14] and in numerical studies for plate systems [15]. It has been highlighted that they exhibit errors around the natural frequencies of the removed subsystem [17]. In the proposed approach, the systems studied can be either mechanical, acoustical, or vibroacoustical, and the response of the system can be obtained at any point of the domain. The validity of the method has already been studied in a previous paper [12], hence this article focuses on the sensitivity of the method when model errors are introduced via the calculation of the Condensed Transfer Functions.

2. PRINCIPLE OF THE REVERSE CTF METHOD

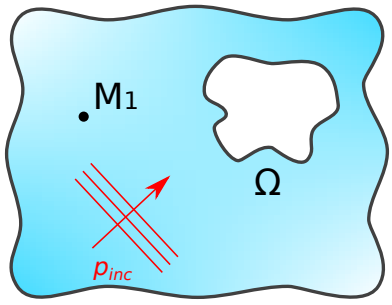

Figure 1: Scattering of a plane wave by a rigid object.

The system of interest of this study is defined in Figure 1, which is the scattering of a plane wave by a rigid object in a fluid medium. This rigid object can be considered as a presence of a void in the medium, and for which we want to study the effect. In order to do so, we can consider the decoupling problem presented in Figure 2.

Let us consider two domains initially coupled along a surface Ω, where the first subsystem is excited by an external force that takes the form of an acoustic plane wave, as illustrated in Figure 2.

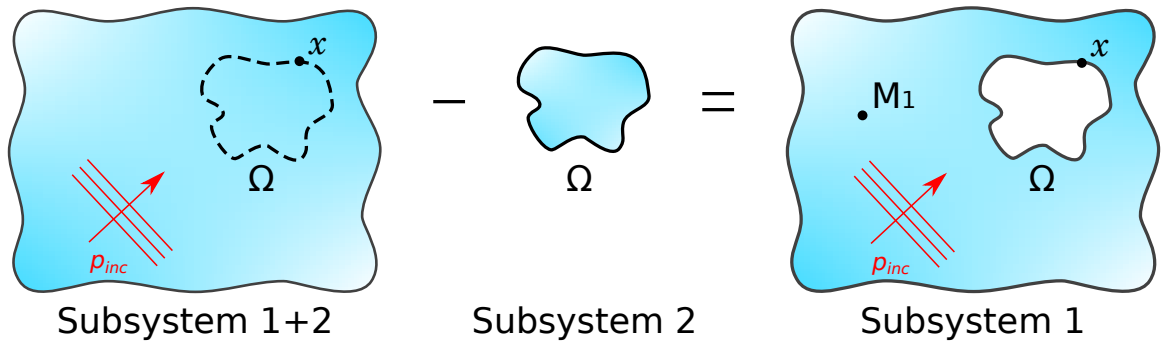

Figure 2: Principle of the reverse CTF method.

The responses are calculated in harmonic regime. We are interested in getting the reponse at any point M_1 of the decoupled subsystem 1. To do so, a set of N orthonormal functions defined on Ω, called the condensation functions, is considered: $\{\varphi^i\}_{1\leq i\leq N}$. For each subsystem α, the pressures p_α and normal velocities u_α at the junction can be approximated as a linear combination of the condensation functions:

$$p_\alpha(x) \simeq \sum_{i=1}^{N} P^i_\alpha \varphi^i(x) \quad \text{and} \quad u_\alpha(x) \simeq \sum_{i=1}^{N} U^i_\alpha \varphi^i(x), \quad x \in \Omega \tag{1}$$

As the theoretical developments of the rCTF method are fully described in [12], a reminder of the quantities that are necessary to apply the method will be given here. These quantities are related to the known subsystems 1+2 and 2.

In order to estimate P^i_α and U^i_α in Eq. (1), condensed transfer functions (CTFs) between φ_i and φ_j are defined for each uncoupled subsystem by applying a prescribed velocity $u_\alpha = \varphi^j$ on Ω:

$$Z^{ij}_\alpha = \frac{\langle \bar{p}_\alpha, \varphi^i \rangle}{\langle u_\alpha, \varphi^j \rangle} = \langle \bar{p}_\alpha, \varphi^i \rangle \tag{2}$$

where $\bar{p}_\alpha$ is the resulting pressure on the junction Ω when the subsystem is excited by $u_\alpha = \varphi^j$, and $\langle \bullet, \bullet \rangle$ is a scalar product. The condensed impedance matrix of subsystem 2, $\boldsymbol{Z_2}$ is hence obtained by this process, as well as the condensed impedance matrix of subsystem 1, $\boldsymbol{Z_1}$. As for subsystem 1+2, the condensed transfer function between φ^i and φ^j is defined by applying a prescribed velocity jump corresponding to φ^j at the junction Ω:

$$Z^{ij}_{1+2} = \frac{P^i_{1+2}}{\delta U^j_{1+2}} = \frac{\left\langle \bar{p}_{1+2}, \varphi^i \right\rangle}{\langle \varphi^j, \varphi^j \rangle} = \left\langle \bar{p}_{1+2}, \varphi^i \right\rangle \tag{3}$$

The other quantities that are necessary to apply this decoupling process are related to subsystem 1+2:

- $p_{1+2}(M_1)$, which is the pressure induced by the plane wave at point M_1 of subsystem 1+2.
- $\boldsymbol{P_{1+2}}$, which is the condensed pressure at the surface Ω of subsystem 1+2 induced by the plane wave.
- $\boldsymbol{P^{M_1}_{1+2}}$, which is the condensed pressure at the surface Ω of subsystem 1+2, induced by a monopole source of unit volume volume velocity located at point M_1.

These quantities allow us to obtain the two necessary informations from the decoupled subsystem 1. The condensed impedance $\boldsymbol{Z_1}$ is given by:

$$\boldsymbol{Z_1} = \boldsymbol{Z_2} \left(\boldsymbol{Z_2} - \boldsymbol{Z_{1+2}} \right)^{-1} \boldsymbol{Z_{1+2}} \tag{4}$$

While the pressure at any point M_1 of the subsystem 1 can be written as:

$$\tilde{p}_1(M_1) = p_{1+2}(M_1) + \left(\boldsymbol{I} + \boldsymbol{Z_2}\left(\boldsymbol{Z_2} - \boldsymbol{Z_{1+2}}\right)^{-1} \boldsymbol{Z_{1+2}} \boldsymbol{Z_2^{-1}}\right) \boldsymbol{P_{1+2}^{M_1}} \boldsymbol{Z_2^{-1}} \boldsymbol{P_{1+2}} \tag{5}$$

where $\boldsymbol{I}$ is the identity matrix.

3. NUMERICAL SIMULATIONS ON A TEST CASE

3.1. Definition of the test case

The rCTF method has already been validated from a theoretical point of view in a previous work [12]. This paper is hence focused on the sensitivity of the method to model errors. In this regard, the rCTF method will be applied on an academic test case consisting in the scattering of an acoustic plane wave by a rigid sphere immersed in an infinite water domain. As illustrated in Figure 3, this test case consists in removing a water sphere (subsystem 2) from an infinite water domain (subsystem 1+2). The result will be the infinite water domain with a rigid sphere at its center (subsystem 1), which is the origin of the coordinates in the spherical coordinate system. The characteristrics of the infinite domain and of the sphere are given in Table 1.

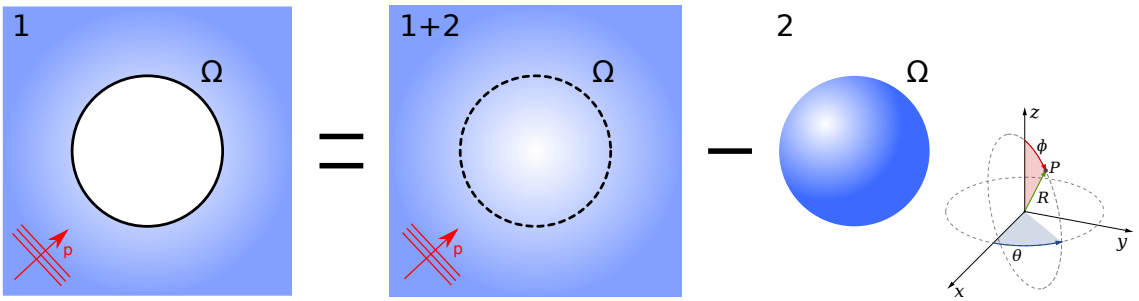

Figure 3: Application of the reverse CTF method to the scattering of a plane wave by a rigid sphere.

Table 1: Material characteristics and dimensions.

Parameter	Notation	Value	Unit
Radius	a	1	m
Density	ρ	1000	kg.m^{-3}
Sound speed	c_0	1500	m.s^{-1}
Loss factor	η	0.001	-

For purposes of comparison, a theoretical reference calculation has been carried out by expanding the incident plane wave and the scattered pressure field in spherical harmonics, and the harmonic responses are calculated in the frequency range [100, 1 000] Hz with 1 Hz steps. In this frequency range lie the first two resonant frequencies (i.e. 497 Hz and 798 Hz) and first anti-resonant frequency (i.e. 750 Hz) of the sphere. In order to apply the rCTF approach, the condensed impedances, as defined in Section 2, can be calculated by different means, either analytical or numerical. These calculations depend on the condensation functions that are considered, as stated in Eq. (2). These condensation functions will be presented in the next section.

3.2. Definition of the condensation functions

In order to apply the rCTF method, the condensation functions must be defined. In this work, the condensation functions that are investigated are the 2D gate functions, defined depending on their surface Ω_s:

$$\varphi^i(\theta_s, \phi_s) = \begin{cases} \frac{1}{\sqrt{\Omega_s}} & \text{if} \quad \begin{cases} \theta_{i-1} \leq \theta_s < \theta_i \\ \phi_{i-1} \leq \phi_s < \phi_i \end{cases} \quad , \quad i \in [\![1, N]\!] \\ 0 \quad \text{elsewhere} \end{cases} \tag{6}$$

These condensation functions are orthonormal following the scalar product at the surface of the sphere in spherical coordinates:

$$\left\langle \varphi^i, \varphi^j \right\rangle = \int_0^{2\pi} \int_{-\pi/2}^{\pi/2} \varphi^i \varphi^{j*} a^2 \sin\theta \, \mathrm{d}\theta \, \mathrm{d}\phi = \delta_{ij}, \tag{7}$$

where δ_{ij} is the Kronecker symbol, and * denotes the complex conjugate. Using 2D gate functions as condensation functions amounts to dividing the sphere into N patches, and the condensed impedance between patches i and j is computed by calculating the mean pressure on patch i when a unit prescribed velocity is imposed on patch j. The definition of the four angles θ_{i-1}, θ_i, ϕ_{i-1} and ϕ_i that appear in Eq. (6) is given in Figure 4a, while the patches at the surface of the sphere are shown in Figure 4b. Following the definition of the PTF method, using these condensation functions can be considered as applying the reverse PTF approach.

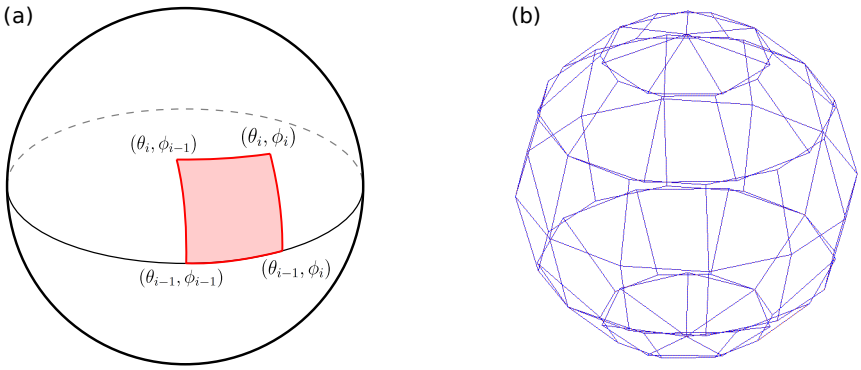

Figure 4: (a) Definition of a patch related to a 2D gate function. (b) Definition of the patches over the sphere surface.

In order for the rCTF method to correctly converge, the size and the number of the patches must be carefully chosen (see [10]). According to previous studies on the PTF and CTF methods, a criterion based on the Nyquist-Shannon sampling theorem has been derived stating that at least two points per wavelength are necessary to sample a signal. Following this recommandation, the acoustic wavelength at the highest frequency of interest (i.e. 1 000 Hz) should be considered, yielding $\lambda_{min} = 1.5$ m. As for the size of the patches, they should be smaller than half the shortest wavelength:

$$d < \frac{\lambda_{min}}{2} \tag{8}$$

The sphere is thus divided into 58 patches as shown in Figure 4b, following the criterion in Eq. (8). It is important to mention that the geometrical particularities of the patches (namely, that the patches at the top and bottom of the sphere are triangular, and that the nodes of two consecutive patches are not necessarily coincident) do not have any influence on the results of the PTF and reverse PTF methods.

3.3. Numerical calculation of the condensed impedances

Once that the condensation functions have been defined, it is necessary to compute the condensed impedances of the different subsystems in order to apply the rCTF method, based on Eqs. (4) and (5). In our previous work [12], the condensed impedances have been calculated by analytical means, in order to validate the method from a theoretical point of view. Hence, as this paper is focused on the sensitivity of the method to model errors, the condensed impedances will be computed using numerical formulations. The analytical calculation can still serve as a reference to evaluate the decoupling of the condensed impedances of Eq. (4).

According to Eq. (4), the condensed impedances of the subsystem 1, which is of interest and corresponds to the rigid sphere in an infinite water medium, are obtained from the condensed impedances of the subsystem 1+2, which is the infinite water domain, and of the subsystem 2, which is the sphere of water. Let us focus at first on the numerical calculation of the condensed impedances of the subsystem 1+2.

(a) *Condensed impedances of the subsystem 1+2*: according to Filippi [18], layer potentials can be used as a solution of the homogeneous Helmholtz equation in an open domain. The pressure at the fictitious surface of the sphere in subsystem 1+2 can hence be expressed using a single layer potential:

$$p(M) = \int_{\Omega} \nu(P) G(M,P)\, \mathrm{d}\Omega(P), \quad M(\theta_M, \phi_M) \in \Omega, \quad P(\theta_P, \phi_P) \in \Omega \tag{9}$$

where $\nu(P)$ is the single layer potential due to a layer of spherical sources and represents a velocity jump at the crossing of the fictitious surface of the sphere. $G(M,P)$ is the Green function and corresponds to the sound field at point M due to a spherical point source located at point P. With the temporal dependency of the problem being $\mathrm{e}^{-\mathrm{i}\omega t}$, it is defined as:

$$G(M,P) = -\frac{\mathrm{e}^{\mathrm{i}k(1-\mathrm{i}\eta)r(M,P)}}{4\pi r(M,P)} \tag{10}$$

with k being the acoustic wavenumber, η the damping loss factor (to account for dissipative effects in the domain) and $r(M,P)$ the distance between points M and P. In order to include this formulation into the rCTF problem to calculate the condensed impedances of the subsystem 1+2, the velocity jump in Eq. (9) must correspond to a condensation function φ^j. Following this, the integration in Eq. (9) must be evaluated numerically. One way to do so is to discretize the integral with a rectangular rule. According to the definition of the condensation functions in Eq. (6), the patch j corresponding to φ^j must be discretized into R_j points between θ_{j-1} and θ_j in the θ dimension and into S_j points between ϕ_{j-1} and ϕ_j in the ϕ dimension. Eq. (9) can then be written:

$$p(M) = \sum_{r_j=1}^{R_j} \sum_{s_j=1}^{S_j} \frac{G(\theta_{r_j} - \theta_M, \phi_{s_j} - \phi_M) \sin\theta_{r_j}}{\sqrt{\Omega_j}} \delta\theta_j \delta\phi_j, \quad \begin{cases} \theta_{r_j} \in [\theta_{j-1}, \theta_j] \\ \phi_{r_j} \in [\phi_{j-1}, \phi_j] \end{cases} \tag{11}$$

where Ω_j is the surface of the patch j, and $\delta\theta_j$ and $\delta\phi_j$ are the discretization step in the θ dimension and ϕ dimension of patch j, respectively. According to the definition of the condensed transfer functions in Eq. (3), the discretized condensed transfer function between patch i and patch j for the subsystem 1+2 is then obtained by projecting the expression in Eq. (11) on the condensation function φ^i. Once again, it is done by discretizing the patch i into R_i points between θ_{i-1} and θ_i in the θ dimension and into S_i points between ϕ_{i-1} and ϕ_i in the ϕ dimension.

$$Z_{1+2}^{ij} = \sum_{r_i=1}^{R_i} \sum_{s_i=1}^{S_i} \sum_{r_j=1}^{R_j} \sum_{s_j=1}^{S_j} \frac{G(\theta_{r_j} - \theta_{r_i}, \phi_{s_j} - \phi_{s_i}) \sin\theta_{r_j} \sin\theta_{r_i}}{\sqrt{\Omega_j \Omega_i}} \delta\theta_j \delta\phi_j \delta\theta_i \delta\phi_i, \quad \begin{cases} \theta_{r_i} \in [\theta_{i-1}, \theta_i] \\ \phi_{r_i} \in [\phi_{i-1}, \phi_i] \end{cases} \tag{12}$$

where Ω_i is the surface of the patch i, and $\delta\theta_i$ and $\delta\phi_i$ are the discretization step in the θ dimension and ϕ dimension of patch i, respectively. The size of the discretization is a key element to have a good balance between good performances and effective computation cost. After a trial and error test, it has been concluded that taking $\delta\theta_j = \delta\phi_j = \delta\theta_i = \delta\phi_i = 2°$ is a good compromise in terms of performances and computation cost. Finally, considering this method, it is important to study the particular case of the direct condensed transfer function, that is when $i = j$. Regarding the definition of the Green function in Eq. (10), a singularity happens when the excited and receiving nodes are the same. A first possiblity to circumvent this issue is to define a criterion of minimal distance ε between two nodes. If the distance between the two nodes is smaller than ε, it is forced into being ε. A second possibility is to approximate this condensed impedance by doing an analogy. The radiation impedance of a circular baffled piston having the same surface as the patch, corresponding to the pressure at the surface of the piston when a uniform vibrating velocity is prescribed, is defined as:

$$Z_R = Z_0 \left(1 - \frac{J_1(2ka_p)}{ka_p} - \mathrm{i}\frac{S_1(2ka_p)}{ka_p} \right) \tag{13}$$

where Z_0 is the acoustic impedance, a_p is the radius of the circular piston, J_1 is the Bessel function of the first kind and S_1 is the Struve function. An analogy of this expression can be done by considering a uniform velocity jump at the surface of a baffled vibrating disk, and the calculation process would lead to the same expression as Eq. (13). Experience has shown that the first solution is more precise but also more time consuming when the discretization is fine (i.e. $\delta\theta < 2°$), while the second solution works quite well no matter the discretization and is very effective in terms of computation cost.

(b) *Condensed impedances of the subsystem 2*: as for the condensed impedances of the subsystem 2, which is the water sphere, a FEM formulation is used. The mesh of the sphere is generated via Altair Hypermesh, with a criterion of at least 6 elements per acoustic wavelength for the highest frequency considered. The mass and stiffness matrices are extracted from the model using the Structural Dynamic Toolbox implemented in Matlab [19]. The FEM formulation that is solved takes the form:

$$\left([K] - \omega^2 [M](1 - 2\mathrm{i}\eta) \right) \{p\} = \{Q\} \tag{14}$$

where $[K]$ and $[M]$ are the acoustic stiffness and mass matrices, respectively, η is the damping loss factor, $\{p\}$ is the output pressure vector, and $\{Q\}$ is the input volume velocity vector. In order to apply this Finite Element formulation to the calculation of the condensed impedances, the input velocity vector on patch j must be the condensation function φ^j. Following this, the input volume velocity vector $\{Q_j\}$ associated to patch j will have N components q_n^j, with N being the number of nodes belonging to the patch j:

$$q_n^j = \frac{\delta S_n}{\sqrt{\Omega_j}}, \quad n \in [\![1, N]\!] \tag{15}$$

where δS_n is the area around the node n. The resulting pressure at each node k of the Finite Element model is then obtained by inverting Eq. (14):

$$p_k = \left([K] - \omega^2 [M](1 - 2\mathrm{i}\eta) \right)^{-1} \{Q_j\} \tag{16}$$

Finally, the condensed transfer function between patch i and patch j is obtained by projecting the pressure in Eq. (16) on the condensation function φ^i. In practice, this projection is carried out via a discrete sum over the M nodes of the Finite Element model belonging to the patch i:

$$Z_2^{ij} = \sum_{m=1}^{M} \frac{p_m}{\sqrt{\Omega_i}} \delta S_m \tag{17}$$

where δS_m is the area around the node m. As for the subsystem 1+2, the mesh size of the Finite Element model is a very important parameter for the computation to be precise enough. As stated before, a criterion of 6 elements per acoustic wavelength is generally used in this kind of studies. However, applying such a criterion was not enough in this case as the resonant and anti-resonant frequencies of the water sphere were not correctly described in this model. A criterion of 15 elements per acoustic wavelength (at the highest considered frequency) was hence retained to be close enough to the analytical calculation: the relative error on the frequency of the highest resonance (i.e. 750 Hz) is 0.13%, against 1.4% for the criterion of 6 elements per acoustic wavelength.

3.4. Decoupling of the condensed impedances

As a first step, to evaluate the sensitivity of the rCTF method to model errors, the calculation of the condensed impedances of subsystem 1, $\boldsymbol{Z_1}$, are computed using $\boldsymbol{Z_{1+2}}$, $\boldsymbol{Z_2}$, and the decoupling formula of Eq. (4). The results are compared to an analytical calculation of $\boldsymbol{Z_1}$ (developpment not shown here). In order to sweep different possibilities of transfer functions (TFs), the comparison is shown for:

- a direct condensed impedance on a trapezoid patch (the excitation and observation patch are the same) - 1st TF.
- a direct condensed impedance on a triangular patch - 2nd TF.
- a crossed condensed impedance between two trapezoid patches that are close to each other - 3rd TF.
- a crossed condensed impedance between a trapezoid patch and a triangular patch that are widely separated one from another - 4th TF.

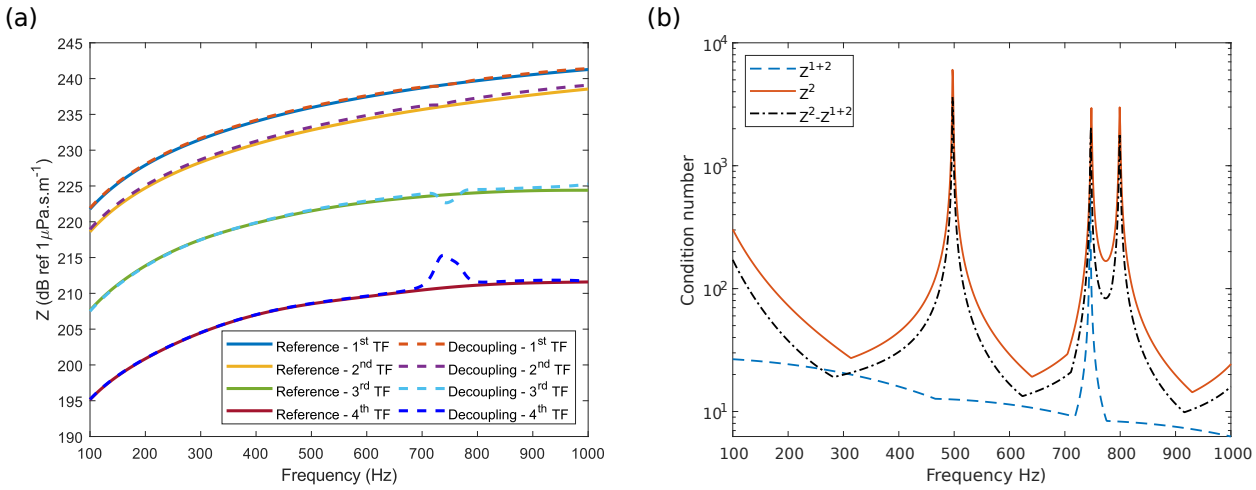

Figure 5: (a) Comparison between the condensed impedances computed analytically and with the rCTF approach. (b) Condition number of the inverted matrix for the three subsystems.

The comparison is shown in Figure 5a, and the results show a relatively good fit between the reference calculation and the rCTF calculation. It can however be seen, especially for the 4th TF, that discrepancies appear around 750 Hz. This frequency corresponds to the anti-resonant frequency of the water sphere, which had already been identified as ill-conditionned in previous studies concerning decoupling procedures [12, 17]. Indeed, the condition number of the inverted matrix ($\boldsymbol{Z_2} - \boldsymbol{Z_{1+2}}$) is particularly high at the resonant and anti-resonant frequencies of the water sphere, as seen on Figure 5b. The introduction of model errors in the calculation of the condensed impedances of subsystems 2 and 1+2 hence amplifies the ill-conditionning around the anti-resonant frequency, which explains

the observed errors. Although the results are not perfect, there is a clear tendancy showing that the numerical decoupling calculation in very close to the reference calculation. Also, we are interested in this study in evaluating the scattering of the plane wave by a rigid sphere, described by Eq. (5). The next sections will hence be focused on the impact of the numerical errors on this calculation.

3.5. Calculation of the condensed pressures

In order to evaluate the decoupling formula of Eq. (5), the condensed pressure $\boldsymbol{P}_{\mathbf{1+2}}^{\boldsymbol{M_1}}$ and $\boldsymbol{P}_{\mathbf{1+2}}$ must also be evaluated by numerical means. It is reminded that $\boldsymbol{P}_{\mathbf{1+2}}^{\boldsymbol{M_1}}$ corresponds to the condensed pressure at the fictitious surface of the sphere of subsystem 1+2 when the excitation is a unitary monopole situated at point M_1. On the other hand, $\boldsymbol{P}_{\mathbf{1+2}}$ is the condensed pressure induced at the fictitious surface of the sphere of subsystem 1+2 when it is impacted by a plane wave. In order to evaluate numerically these condensed pressures, the surface of the sphere is discretized using the same process as for the condensed impedances of subsystem 1+2.

(a) *Condensed pressure induced by a unitary monopole*: the acoustic pressure field at any point $M(R, \theta, \phi)$ of a fluid domain induced by a monopole of unit volume velocity located at point $M_1(R_1, \theta_1, \phi_1)$ can be expressed using the free space Green function defined in Eq. (10):

$$p_i^{M_1} = \mathrm{i}\omega\rho G(M, M_1) \tag{18}$$

The condensed pressure is then obtained by evalutating the pressure of Eq. (18) at the surface of the sphere and projecting it on the condensation function φ^i. In practice, this pressure is evaluated at each discretization point belonging to the patch i and summed over the patch:

$$P_{1+2,i}^{M_1} = \mathrm{i}\omega\rho \sum_{r_i=1}^{R_i} \sum_{s_i=1}^{S_i} \frac{G(\theta_{r_i} - \theta_{M_1}, \phi_{s_i} - \phi_{M_1})}{\sqrt{\Omega_i}} \sin\theta_{r_i} \delta\theta_i \delta\phi_i, \quad \begin{cases} \theta_{r_i} \in [\theta_{i-1}, \theta_i] \\ \phi_{r_i} \in [\phi_{i-1}, \phi_i] \end{cases} \tag{19}$$

As for the condensed impedances of subsystem 1+2, this formulation can exhibit a singularity when the monopole is located at the surface of the sphere. When such a phenomenon appears, a criterion of minimal distance, as described before, is then retained.

(b) *Condensed pressure induced by an acoustic plane wave*: the acoustic pressure field of a plane wave of angular frequency ω travelling in the direction $(\theta = \pi, \phi = 0)$ is defined by:

$$p_i(R, \theta) = P_i \mathrm{e}^{ik_0 R\cos\theta} \tag{20}$$

where P_i is the amplitude of the plane wave and k_0 the acoustic wavenumber. Similarly to the previous calculation, the condensed pressure is obtained by evaluating the pressure in Eq. (20) at the surface of the sphere and projecting it on the condensation function φ^i. For a patch i discretized into R_i points between θ_{i-1} and θ_i in the θ dimension and into S_i points between $\phi i - 1$ and ϕ_i in the ϕ dimension, it yields:

$$P_{1+2,i} = P_i \sum_{r_i=1}^{R_i} \sum_{s_i=1}^{S_i} \frac{\mathrm{e}^{ik_0 R\cos\theta_{r_i}}}{\sqrt{\Omega_i}} \sin\theta_{r_i} \delta\theta_i \delta\phi_i, \quad \theta_{r_i} \in [\theta_{i-1}, \theta_i] \tag{21}$$

3.6. Computation of the pressure in the domain

Now that all the quantities that are necessary to calculate Eq. (5) have been obtained, we can focus on evaluating the sensitivity of the method when numerical errors have been introduced in the models. In order to do so, the decoupling formula of Eq. (5) will be compared to reference calculation based

on the expansion in spherical harmonics of the plane wave and the scattered field. This theoretical development yields, for any point in the domain:

$$p_{theo}(R,\theta) = P_i \sum_{n=0}^{+\infty} (2n+1)\mathrm{i}^n P_n(\cos\theta)\left[j_n(k_0 R) - \frac{j_n'(k_0 a) h_n(k_0 R)}{h_n'(k_0 a)} \right] \tag{22}$$

where P_i is the amplitude of the plane wave, $P_n(\cos\theta)$ is the Legendre polynomial, j_n and j_n' are the spherical Bessel function of the first kind and its derivative, and h_n and h_n' are the spherical Hankel function of the first kind and its derivative. In practice, this expression must be truncated to a maximum number N of spherical harmonics. After a trial and error test, the calculation has correctly converged in the frequency band of interest for $N = 40$ harmonics.

A first way of evaluating the rCTF calculation for the scattering of a plane wave by a rigid sphere is to observe the evolution of the pressure over the frequency range at a single point of the domain. The comparison between the theoretical calculation and the decoupling one is shown in Figure 6 for 3 different points in the fluid domain to account for different possibilities in terms of distance to the surface of the sphere and of angular orientation. The quantity that is plotted here is the sound pressure level, with a reference pressure $p_0 = 1\mu Pa$.

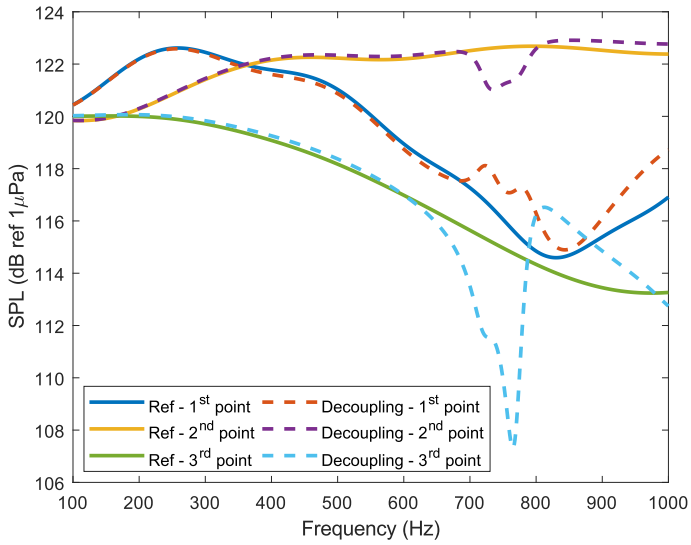

Figure 6: Pressure scattered by the rigid sphere - evaluation of the decoupling for 3 points in the fluid domain. Point 1 - $r = 1.5$ m, $\theta = 180°$; Point 2 - $r = 1.3$ m, $\theta = 103°$; Point 3 - $r = 1$ m, $\theta = 30°$.

As could be expected from the calculation of the condensed impedances discussed in Section 4, the calculation of the decoupled pressure exhibits errors that are mainly situated around the anti-resonant frequency of the water sphere. One can also notice that these errors seem to be higher when the pressure is observed at the surface of the sphere. Even if a criterion was established to circumvent the singularities that can happen when the monopole is situated at the surface of the sphere, the high values exhibited by monopoles at such short distances may be prohibitive. However, we can emphasize that in most parts of the frequency range of the calculation the decoupling can be considered as very effective. In order to validate this statement, a cartography of the scattered pressure field around the rigid sphere can be plotted for several frequencies.

The cartography of the scattered pressure field for the two calculations is shown in Figure 7. Figures (a) and (c) correspond to the reference calculation while the results of the decoupling calculation are shown in Figures (b) and (d). As stated above, at 600 Hz (corresponding to Figures (a) and (b)), there is no apparent error as this frequency showed no particular problem previously. As a comparison, in Figures (c) and (d) are plotted the results at 750 Hz, the ill-conditionned frequency

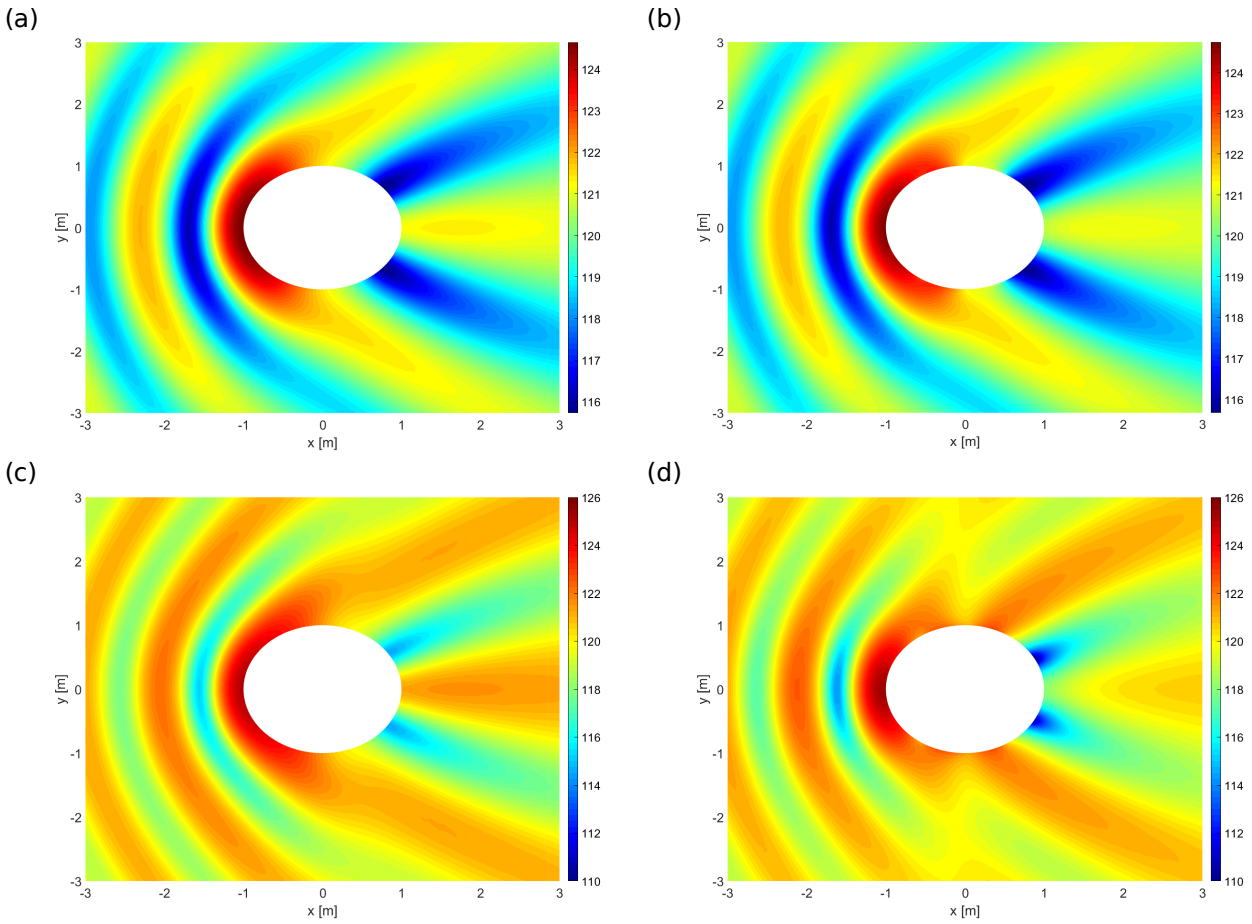

Figure 7: Pressure scattered by the rigid sphere - Comparison between theoretical results (a,c) and decoupling results (b,d) for 2 frequencies: (a,b) 600 Hz; (c,d) 750 Hz.

which corresponds to the anti-resonance of the water sphere. However, even at this frequency, if there are some discrepancies, one can observe that the global behavior stays well described by the decoupling process, as the maxima and minima of pressure are correctly located.

4. CONCLUSIONS

After having been validated from an analytical point of view, the reverse Condensed Transfer Function method has been applied to a test case in order to evaluate its sensitivity to model errors. To this end, the condensed impedances and pressures necessary to apply the method have been computed by numerical means. A discrete Green formulation has been used for the infinite water medium, while the condensed impedances of the water sphere have been computed via a Finite Element formulation.

It has been shown that the method is particularly sensitive to errors around the anti-resonant frequency of the subtracted subsystem, which was the water sphere, following the conclusions previously drawn on decoupling procedures. The precision of the numerical models used to compute the condensed impedances could hence be improved, resulting however in a substantial increase in the computation time. Also, this decoupling method could be associated to a direct method to couple a model of an elastic sphere, for example, hence potentially reducing the sensitivity of the method. Finally, one has to keep in mind that a higher damping loss factor would strengthen the accuracy of the method as it has been proven before.

The results of this study give a good overview of the potential advantages and drawbacks of the rCTF method, and give insight on its applicability to industrial cases.

ACKNOWLEDGEMENTS

This work was funded by Naval Group Research and performed within the framework of the LabEx CeLyA (ANR-10-LABX-0060) of Université de Lyon, within the program "Investissements d'Avenir" (ANR-16-IDEX-0005) operated by the French National Research Agency (ANR).

REFERENCES

[1] F.A. Firestone. The mobility method of computing the vibration of linear mechanical and acoustical systems: mechanical-electrical analogies. *J. Appl. Phys.*, 9(6):373–387, 1938.

[2] S. Rubin. Transmission matrices for vibration and their relation to admittance and impedance. *J. Eng. Ind.*, 86(1):9–21, 1964.

[3] G.J. O'Hara. Mechanical impedance and mobility concepts. *J. Acoust. Soc. Am.*, 41(5):1180–1184, 1967.

[4] B. Petersson and J. Plunt. On effective mobilities in the prediction of structure-borne sound transmission between a source structure and a receiving structure, part II: Procedures for the estimation of mobilities. *J. Sound Vib.*, 82(4):531–540, 1982.

[5] S.M. Kim and M.J. Brennan. A compact matrix formulation using the impedance and mobility approach for the analysis of structural-acoustic systems. *J. Sound Vib.*, 223(1):97–113, 1999.

[6] L. Maxit, C. Caccioliti, and J.-L. Guyader. Airborne noise prediction using patch acoustic impedance. In *Proceedings of ICSV 9*, Orlando, United States, 2002.

[7] M. Ouisse, L. Maxit, C. Cacciolati, and J.-L. Guyader. Patch transfer function as a tool to couple linear acoustic problems. *J. Vib. Acoust.*, 127:pp. 458–466, 2005.

[8] L. Maxit, M. Aucejo, and J.-L. Guyader. Improving the Patch Transfer Function approach for fluid-structure modelling in heavy fluid. *J. Vib. Acoust.*, 134(5):051011, 2012.

[9] M. Aucejo, L. Maxit, N. Totaro, and J.-L. Guyader. Convergence acceleration using the residual shape technique when solving structure–acoustic coupling with the Patch Transfer Functions method. *Comput. Struct.*, 88(11):728–736, 2010.

[10] V. Meyer, L. Maxit, J.-L. Guyader, T. Leissing, and C. Audoly. A condensed transfer function method as a tool for solving vibroacoustic problems. *Proceedings of the Institution of Mechanical Engineers, Part C: J. Mech. Eng. Sci.*, 230(6):928–938, 2016.

[11] V. Meyer, L. Maxit, J.-L. Guyader, and T. Leissing. Prediction of the vibroacoustic behavior of a submerged shell with non-axisymmetric internal substructures by a condensed transfer function method. *J. Sound Vib.*, 360:260–276, 2016.

[12] F. Dumortier, L. Maxit, and V. Meyer. Vibroacoustic subtractive modeling using a reverse condensed transfer function approach. *J. Sound Vib.*, 499:115982, 2021.

[13] D. T. Soedel and W. Soedel. Synthesizing reduced systems by complex receptances. *J. Sound Vib.*, 179(5):855 – 867, 1994.

[14] W. D'Ambrogio and A. Fregolent. Decoupling of a substructure from modal data of the complete structure. In *Proceedings of ISMA2004: International Conference on Noise and Vibration Engineering*, Leuven, Belgium, 2004.

[15] D. T. Huang and E. C. Ting. Vibration of plates with sub-structural deduction: a reverse receptance approach. *J. Sound Vib.*, 271(1-2):177–207, 2004.

[16] W. D'Ambrogio and A. Fregolent. Promises and pitfalls of decoupling procedures. In *26th IMAC: Conference and Exposition on Structural Dynamics*, Orlando, United States, 2008.

[17] P. J. T. Filippi. Layer potentials and acoustic diffraction. *J. Sound Vib.*, 54(4):473–500, 1977.

[18] SDTools. *Structural Dynamics Toolbox (for use with MATLAB)*. Paris, 1995-2020.